Pis'ma v ZhETF, vol. 86, iss. 8, pp. 616 – 620

Microwave induced magnetoresistance oscillations at the subharmonics of the cyclotron resonance

S. I. Dorozhkin[1)], *J. H. Smet*+, *K. von Klitzing*+, *L. N. Pfeiffer**, *K. W. West**

Institute of Solid State Physics, 142432 Chernogolovka, Moscow district, Russia

+ *Max-Planck-Institut für Festkörperforschung, D-70569 Stuttgart, Germany*

**Bell Laboratories, Lucent Technologies, Murray Hill, New Jersey 07974*

Submitted 4 September 2007

The magnetoresistance oscillations, which occur in a two-dimensional electron system exposed to strong microwave radiation when the microwave frequency ω coincides with the *n-th* subharmonic of the cyclotron frequency ω_c, have been investigated for $n = 2, 3$ and 4. It is shown that these subharmonic features can be explained within a non-equilibrium energy distribution function picture without invoking multi-photon absorption processes. The existence of a frequency threshold above which such oscillations disappear lends further support to this explanation.

PACS: 72.20.–i, 73.40.Kp

The observation of microwave induced magnetoresistance oscillations (MIMO) with some minima approaching zero resistance in state-of-the-art two-dimensional electron systems (2DES) [1 – 3] has attracted great interest. The effect is governed by the ratio of the circular microwave frequency to the cyclotron frequency: ω/ω_c. At magnetic fields B close to an integer ratio, i.e. at the cyclotron resonance (CR) and its harmonics, the magnetoresistance R_{xx} remains unaffected by the microwave radiation (zero-response node). Away from integer ratios, the microwaves cause a drop of R_{xx} at slightly larger ratios, while at smaller values they produce a positive contribution. The two mainstream approaches to explain these oscillations are based on scattering assisted indirect optical transitions [4, 5] and on the creation of a non-equilibrium electron energy distribution function [6, 7]. There is consensus that the negative magnetoresistivity in the MIMO minima predicted by both theories at high microwave power is not seen in experiment, because the system becomes unstable and an inhomogeneous current distribution develops. This current rearrangement yields zero resistance across adjacent voltage probes [8]. Already in early experiments [2, 6, 9], additional oscillations were detected near $\omega = \omega_c/2$ as well as close to other fractional values of ω/ω_c such as 3/2, 5/2, and 2/3. In a recent article [10], these 'fractional' oscillations were tentatively ascribed to multi-photon processes involving the simultaneous absorption of n photons. Here, $n = 2$ or 3 and corresponds to the denominator of the fractional value. This interpretation was supported within the model of microwave induced indirect transitions when multi-photon absorption is included [11 – 13].

In this paper, we report on the observation of MIMO at the subharmonics of ω_c, i.e. when $\omega = \omega_c/n$ with $n = 2, 3$ and 4. In particular, we investigate the frequency ranges where these additional oscillations are observed. We find that they only occur below an n-dependent threshold frequency. If interpreted in terms of indirect optical transitions our data would imply the involvement of two-, three- and four-photon absorption processes. However within this framework, it is difficult to account for the frequency thresholds. We show that all important properties of these additional oscillations, including the n-dependent frequency thresholds, are captured by the non-equilibrium electron distribution function picture when only single-photon absorption is considered.

These studies were done on a modulation doped GaAs/AlGaAs quantum well with an electron density of $n_s = 2.7\cdot10^{11}\,\mathrm{cm}^{-2}$ and a mobility $\mu = 17\cdot10^6\,\mathrm{cm}^2/\mathrm{V\,s}$ corresponding to a transport (momentum relaxation) time $\tau_{tr} = 6.5\cdot10^{-10}\,$s. Hall bars were prepared with a width W of 400 μm. The sample was placed near the end of a short circuited microwave waveguide with a cross-section of $16\times8\,\mathrm{mm}^2$. Waveguide and sample were submerged in liquid ^{3}He, so that a base temperature of 0.4 K was reached when pumping the ^{3}He and 1.4 K when not pumping. To control the microwave power incident on the sample, a carbon resistor was mounted close to it. The dissipative (ρ_{xx}) and Hall (ρ_{xy}) resistivity components were measured with lock-in detection

[1)]e-mail: dorozh@issp.ac.ru

using a 9.3 Hz sinusoidal current of 1 μA or less, which ensured ohmic conditions.

Fig.1 illustrates how the MIMO near $\omega = \omega_c/n$ arise with increasing microwave power measured at the oscillator output. At small power levels, only the MIMO at

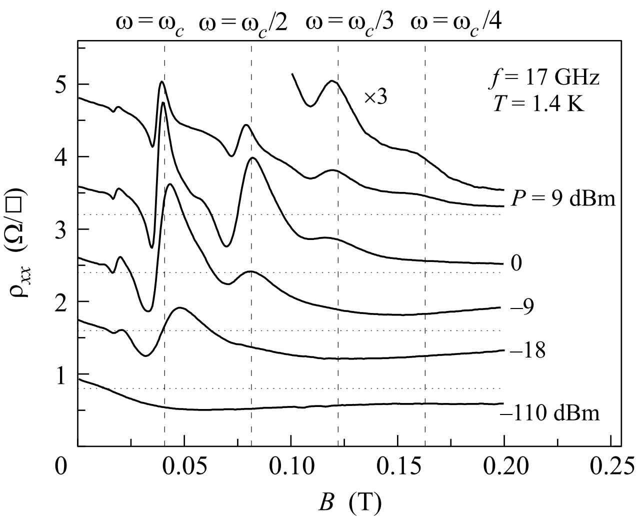

Fig.1. The resistivity ρ_{xx} versus B-field for different microwave power levels at a bath temperature of 1.4 K and a microwave frequency of 17 GHz. For clarity, the curves are offset vertically. The horizontal dotted lines mark zero resistance levels for the shifted curves. Vertical dashed lines indicate the position of the CR and its subharmonics calculated for $m^* = 0.067\, m_e$. To bring out better the microwave induced oscillation at the 4th subharmonic, part of the upper curve has been magnified

the harmonics of ω_c (when $\omega = n\omega_c$) are observed at small B. For example, the curve for $P = -18$ dBm reveals two oscillations located near $\omega = \omega_c$ and $\omega = 2\omega_c$. With increasing power, oscillations emerge at $\omega = \omega_c/n$. At the highest incident power of 9 dBm, the $n = 4$ subharmonic can be discerned. The amplitudes of all MIMO do not change monotonically with power, but pass through a maximum.

Fig.2 demonstrates the existence of zero-response nodes near the location of the cyclotron resonance and its second subharmonic. There, ρ_{xx} does not depend on the microwave power and hence curves recorded at different power levels intersect (for MIMO at $\omega = n\omega_c$ these nodes were considered in some detail in Refs. [1, 14]). Similar nodes do not seem to exist at higher order subharmonics ($n = 3, 4$) and the photoresistivity lies entirely underneath the dark curve ($P = -110$ dBm-trace). Note that both the zero response nodes and the oscillations associated with the 3rd and 4th subharmonic are shifted to a slightly lower B-field than calculated from $\omega = \omega_c/n$ ($n = 1, 2, 3, 4$) when

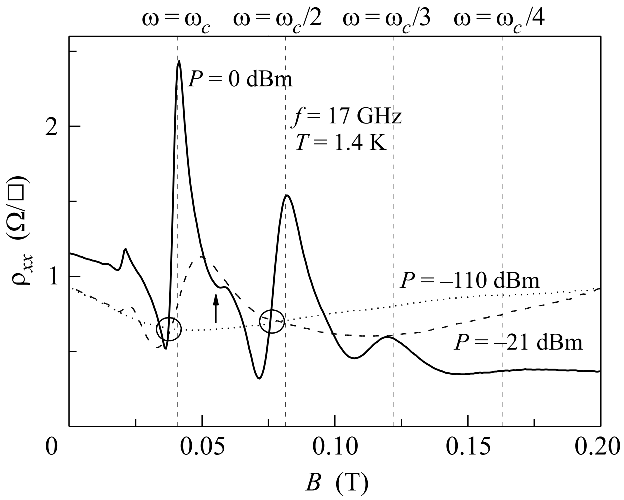

Fig.2. The resistivity ρ_{xx} versus B for different microwave powers as in Fig.1 but without vertical offsets. All curves intersect at the zero-response nodes marked by circles

using the electron effective mass $m^* = 0.067m_e$. The minimum and maximum of each oscillation come closer to the node at larger microwave power. This has also been observed previously for MIMO near $\omega = n\omega_c$ (for example in Ref. [6]). In Fig.2, the minimum located near $\omega = 2\omega_c/3$ becomes visible at the highest power and has been marked by an arrow.

A crucial property of the MIMO at the CR subharmonics is that they are only observed below certain threshold frequencies. In Fig.3 some traces taken at dif-

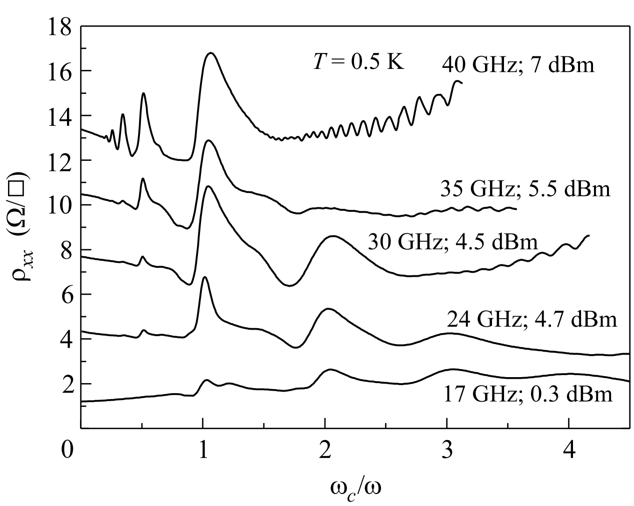

Fig.3. The resistivity ρ_{xx} versus ω_c/ω for different microwave frequencies. Curves were offset for clarity. The microwave power at the waveguide entrance was adjusted to maintain a constant bolometer signal

ferent frequencies are compared. In these experiments, the oscillator output power was adjusted at each frequency to ensure the same bolometer signal. The oscillation near $\omega = \omega_c/2$ appears rather abruptly below 40 GHz. The oscillation is absent at 40 GHz, present at 35 GHz and has drastically increased in amplitude at 30 GHz. Similarly, the threshold frequencies for the 3rd and the 4th subharmonic oscillation lie below 30 and 24 GHz, respectively. Note that in Ref. [2] it was also reported that the second subharmonic feature is only visible below 50 GHz. The amplitudes of the MIMO at harmonics of ω_c ($\omega = n\omega_c$) behave differently. In the investigated frequency regime, they come out stronger at higher frequencies. A careful study with a smaller frequency step than in Fig.3 provides further support for the existence of a frequency threshold and indicates that this effect can not be explained by a variation of the number of modes supported by the waveguide when the frequency is changed.

We will show below in detail that single photon processes are capable of accounting for oscillations at B-fields where ω coincides with a subharmonic of ω_c. First however we discuss the origin of the threshold frequency. Qualitatively MIMO appear within the non-equilibrium occupation picture as a result of transitions between two different broadened Landau levels [6]. Such inter-level transitions are possible provided that $\omega > \omega_c - 2\Gamma/\hbar$ with Γ being the half-width of a Landau level (spin-splitting is neglected in view of the low B-fields). For a B-field at which $\omega = \omega_c/n$, this inequality reduces to $\omega_c(1 - 1/n) < 2\Gamma/\hbar$. This condition is fulfilled only below a certain, sample- and n-dependent threshold magnetic field $B_{\rm th}^{(n)}$ because of the disparate functional dependencies of ω_c and Γ on B: ω_c is proportional to B whereas Γ exhibits a weaker dependence (for example, in the self-consistent Born approximation for non-overlapping Landau levels, i.e. when $\hbar\omega_c > 2\Gamma$: $\Gamma = \hbar\sqrt{2\omega_c/\pi\tau_q} \propto \sqrt{B}$ [15, 16]). Here τ_q is the quantum scattering time. Above this threshold field $B_{\rm th}^{(n)}$, inter-Landau level transitions at the position of the n-th subharmonic are not possible and no oscillation arises. The corresponding frequency threshold $f_{\rm th}^{(n)}$ equals $\omega_c(B_{\rm th}^{(n)})/2\pi n$. It drops with increasing n in agreement with the data presented in Fig.3. If the probability of n-photon processes would be sufficiently high, transitions between neighboring Landau levels would take place at all microwave frequencies, because initial and final states separated by an energy $n\hbar\omega$ close to $\hbar\omega_c$ would be available and there would be no threshold frequency. The inset to Fig.5 covers the special case when $n = 2$. With increasing microwave frequency and B-field, $\Gamma/\hbar\omega_c$ diminishes and the single-photon absorption disappears while the two-photon inter-Landau level transitions do not change qualitatively. Hence, for $f > f_{\rm th}^{(2)}$ a photoresponse caused by single-photon processes is absent all together for B-fields where $\omega \approx \omega_c/2$. This has been demonstrated previously in Ref. [17]. Here, this 'zero response'-region appears at approximately 40 GHz and indeed the MIMO at the second subharmonic develops only at lower frequencies (see Fig.3). If two-photon processes would play a significant role such an effect would not take place. With the above considerations, $f_{\rm th}^{(2)}$ can be written as $\Gamma(B_{\rm th}^{(2)})/\pi\hbar$ and reduces in the self-consistent Born approximation to $f_{\rm th}^{(2)} = (2/\pi)\sqrt{2f_{\rm th}^{(2)}/\tau_{\rm q}}$. Hence, from the threshold frequency the quantum scattering time τ_q can be determined. For $f_{\rm th}^{(2)} = 40\,\rm GHz$ we obtain $\tau_{\rm q} = 2\cdot 10^{-11}\,\rm s \ll \tau_{\rm tr}$.

The estimated value of $\tau_{\rm q}$ implies that the features at the subharmonics of ω_c in Fig.1 and 2 exist in a regime where the Landau levels are separated. Hence, we will consider separated Landau levels in our theoretical calculations based on a non-equilibrium electron distribution function. For the dc diagonal conductivity $\sigma_{\rm xx}^{\rm dc}$ under microwaves we adopt the following formula from Refs. [6] and [7]:

$$\sigma_{\rm xx}^{\rm dc} = \int \sigma(\epsilon)\left(-\frac{\partial f}{\partial \epsilon}\right) d\epsilon. \quad (1)$$

Here $\sigma(\epsilon)$ equals $\frac{n_s e^2 \tau_{\rm tr}}{m^*(\omega_c\tau_{\rm tr})^2}\tilde{\nu}^2(\epsilon)$, $\tilde{\nu}(\epsilon) = \nu(\epsilon)/(m^*/\pi\hbar^2)$ is the density of states in a quantizing B-field normalized to its $B = 0$-value and $f(\epsilon)$ is a steady state non-equilibrium distribution function. The solution of the kinetic equation within the energy relaxation time approximation yields the following recursive formula for $f(\epsilon)$ [7]:

$$P_\omega \sum_{\pm} \tilde{\nu}(\epsilon \pm \hbar\omega)[f(\epsilon \pm \hbar\omega) - f(\epsilon)] = f(\epsilon) - f_T(\epsilon), \quad (2)$$

where f_T is the Fermi distribution function. The dimensionless quantity P_ω is a measure for the incident microwave power and is given by

$$P_\omega = \frac{\tau_{\rm in}}{4\tau_{\rm tr}}\left(\frac{eE_\omega v_{\rm F}}{\hbar\omega}\right)^2 \frac{\omega_c^2 + \omega^2}{(\omega^2 - \omega_c^2)^2}. \quad (3)$$

Here, $\tau_{\rm in}$ is the energy relaxation time of photo-excited electrons, E_ω is the amplitude of the microwave electric field, and $v_{\rm F}$ is the Fermi velocity. The resistivity $\rho_{\rm xx}$ equals $\sigma_{\rm xx}/\sigma_{\rm xy}^2$ with $\sigma_{\rm xy} = n_s e/B$. The non-equilibrium distribution function theory in Ref. [7] has been developed within the self-consistent Born approximation and the density of states of a separated Landau level ($\hbar\omega_c > 2\Gamma$) takes on a semi-elliptical form:

$$\nu(\epsilon)=(2N_0/\pi\Gamma)\sum_{n=0}\mathrm{Re}\left[1-\left(\frac{\epsilon-(n+1/2)\hbar\omega_c}{\Gamma}\right)^2\right]^{1/2}. \quad (4)$$

Here, $N_0 = eB/h$ denotes the Landau level degeneracy. Numerical results based on Eqs. (1)–(4) are depicted in Fig.4. They demonstrate the existence of MIMO at the

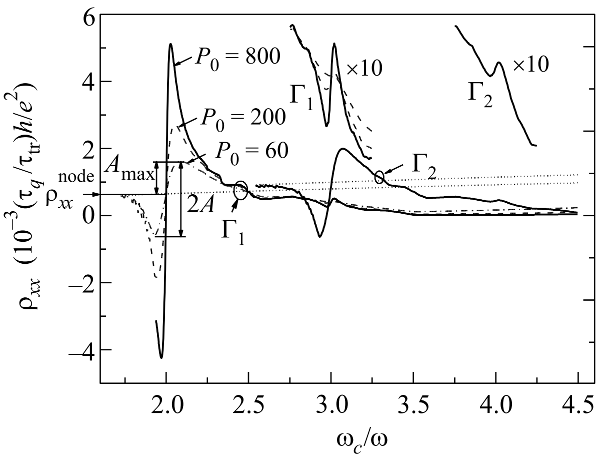

Fig.4. Calculated ρ_{xx} versus ω_c/ω for different power levels $P_0 \equiv P_\omega(\omega_c = 0)$ and two different Landau level widths Γ. The calculations were performed with the following parameter values: $\hbar\omega \approx 6.4\cdot10^{-3}\epsilon_F^0$, $T \approx 1.2\cdot10^{-2}\epsilon_F^0$, $\Gamma_1 \approx \hbar\sqrt{0.45\omega\omega_c}$ and $\Gamma_2 \approx \hbar\sqrt{0.7\omega\omega_c}$. Here ϵ_F^0 is the Fermi energy at $B = 0$, T is the temperature. The right axis shows ρ_{xx} values obtained when using τ_q and τ_{tr} determined as described in the text

second, third and fourth subharmonic of ω_c [18]. These curves reproduce the following experimental features: (i) the shape of the MIMO observed in the experiment, (ii) the existence of a zero-response node near $\omega = \omega_c/2$ where ρ_{xx} is insensitive to the radiation, (iii) the appearance of the 3rd and 4th subharmonic features below the dark curve, and (iv) the large microwave power levels required to make features at the higher order subharmonics appear. As discussed in the introduction, negative resistivity appearing in some MIMO minima turns the system unstable.

Additional support for our interpretation comes from a power dependent study of the amplitude of the oscillation at $\omega = \omega_c/2$. In Fig.5 we compare experimental and theoretical values of two dimensionless quantities $2A/\rho_{xx}^{node}$ and A_{max}/ρ_{xx}^{node}, which are defined in Fig.4. The normalization allows for a straightforward comparison. The only fitting parameter in Fig.5 is a constant coefficient relating the microwave power P measured at

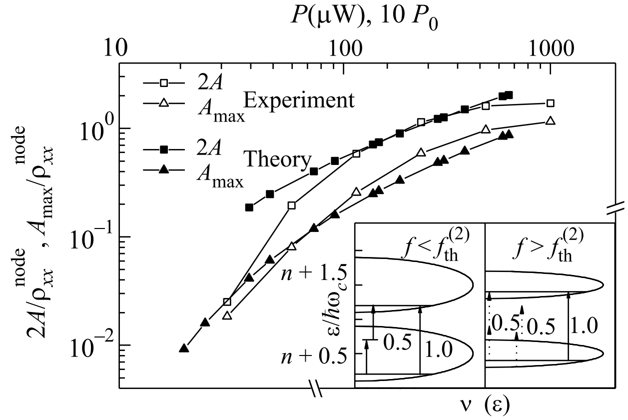

Fig.5. Measured (open signs) and calculated (solid signs) values of A_{max} (triangles) and the total amplitude $2A$ (squares) of the microwave induced oscillation at $\omega = \omega_c/2$ versus the microwave oscillator power P or the dimensionless parameter P_0, respectively. The amplitudes are normalized to the corresponding ρ_{xx} value at the node ρ_{xx}^{node}. The P_0-scale was adjusted to get the best agreement between calculated and measured data for $2A$. The parameters of the calculations are the same as for Fig.4 and $\Gamma = \Gamma_1$. In the insets, broadened Landau levels with semielliptical density of states ν are shown for two magnetic field values. The solid (dotted) arrows depict allowed (forbidden) electron transitions caused by single- (arrows of $0.5\hbar\omega_c$ length) and two-photon (arrows of $1\hbar\omega_c$ length) absorption for a microwave frequency f below (left) and above (right) the threshold frequency $f_{th}^{(2)}$

the oscillator output to the power P_0 used in the calculations. This parameter does not affect the slopes of the curves. Reasonable agreement, in particular when $2A/\rho_{xx}^{node}$ is close to unity, is obtained without any fitting parameters between the experimental and theoretical slopes determined from the normalized amplitude of the subharmonic features.

We conclude that analogous to the MIMO at the harmonics of the cyclotron resonance ($\omega_c = \omega/n$), the subharmonic oscillations at $\omega_c = n\omega$ studied here are related to the *formal* possibility of transferring an electron between equivalent (*separated by the energy* $\hbar\omega_c$) states of two different Landau levels. However as opposed to the harmonics, these subharmonic oscillations are brought about by microwave quanta which constitute only a fraction of the cyclotron energy. Even though the inclusion of multi-photon absorption would allow to extend any of the mechanisms that have been invoked to explain the oscillations at the harmonics of ω_c to the subharmonic oscillations, such a multi-photon picture would contradict the existence of threshold frequencies above which subharmonic oscillations disappear as observed in the experiments described here. Therefore, the role of multi-photon processes, if any, appears only secondary here. If only single-photon absorption and emission processes are allowed, intra-level transitions are capable of setting up a steady-state non-equilibrium distribution function such that single-photon transitions between neighboring levels can take place at any filling of the lower level (see the left panel of the inset to Fig.5). Hence, both intra-level and inter-level transitions are required and work together to produce the subharmonic oscillations. We supported this assertion with theoretical calculations. We note that this distribution function scenario with single-photon absorption/emission can also account for microwave induced features at fractional ratios of ω/ω_c with a nominator different from unity [19].

We acknowledge financial support from INTAS, RFBR (SID) and the DFG. We also thank I. Dmitriev for fruitful comments on the manuscript.

1. R. G. Mani, J. H. Smet, K. von Klitzing et al., Nature **420**, 646 (2002).
2. M. A. Zudov, R. R. Du, L. N. Pfeiffer, and K. W. West, Phys. Rev. Lett. **90**, 046807 (2003).
3. M. A. Zudov, R. R. Du, J. A. Simmons, and J. L. Reno, Phys. Rev. B **64**, 201311(R) (2001).
4. V.I. Ryzhii, Phizika Tverdogo Tela **11**, 2577 (1969) (Sov. Phys. – Solid State **11**, 2078 (1970)).
5. A. C. Durst, S. Sachdev, N. Read, and S. M. Girvin, Phys. Rev. Lett. **91**, 086803 (2003).
6. S. I. Dorozhkin, Pis'ma v ZhETF **77**, 681 (2003) (JETP Lett. **77**, 577 (2003)); cond-mat/0304604.
7. I. A. Dmitriev, M. G. Vavilov, I. L. Aleiner et al., Phys. Rev. B **71**, 115316 (2005).
8. A. V. Andreev, I. L. Aleiner, and A. J. Millis, Phys. Rev. Lett. **91**, 056803 (2003).
9. M. A. Zudov, Phys. Rev. B **69**, 041304(R) (2004).
10. M. A. Zudov, R. R. Du, L. N. Pfeiffer, and K. W. West, Phys. Rev. B **73**, 041303(R) (2006).
11. X. L. Lei and S. Y. Liu, Phys. Rev. Lett. **91**, 226805 (2003).
12. X. L. Lei and S. Y. Liu, Phys. Rev. B **72**, 075345 (2005); cond-mat/0601629.
13. W. Apel, Yu. A. Bychkov, and M. Weyrauch, cond-mat/0512452.
14. R. G. Mani, J. H. Smet, K. von Klitzing et al., Phys. Rev. Lett. **92**, 146801 (2004).
15. T. Ando, A. B. Fowler, and F. Stern, Rev. Mod. Phys. **54**, 437 (1982).
16. I. A. Dmitriev, A. D. Mirlin, and D. G. Polyakov, Phys. Rev. Lett. **91**, 226802 (2003).
17. S.I. Dorozhkin, J.H. Smet, K. von Klitzing, and V. Umansky, Phys. Rev. B **71**, 201306(R) (2005).
18. To illustrate MIMO at the 2nd, 3rd and 4th subharmonic of ω_c, two different Γ are considered: Γ_1 and Γ_2. Due to the assumed $\sqrt{B}$-dependence of the Landau-level width, it is not possible that inter-Landau level transitions are allowed at the 4th subharmonic while simultaneously having separated Landau levels at fields corresponding to the 2nd subharmonic. Hence under the assumption of separated levels, it is not possible to simultaneously obtain MIMO at these two subharmonics for one and the same choice of parameter Γ.
19. I. V. Pechenezhskii, S. I. Dorozhkin, and I. A. Dmitriev, Pis'ma v ZhETF **85**, 94 (2007).